# Kinetics of the Ag/KNO<sub>3</sub>/CaCO<sub>3</sub> Catalyzed Aerobic Propylene Epoxidation and Effects of CO<sub>2</sub>

Sarah E. Specht,<sup>a</sup> Somphonh P. Phivilay,<sup>a</sup> Alessandro Chieregato,<sup>a</sup> Sandor Nagy,<sup>b</sup> Barbara F. M. Kimmich,<sup>b</sup> Ive Hermans <sup>[a,c]\*</sup>

[a] Dr. S. E. Specht, Dr. S. P. Phivilay, Dr. A. Chieregato, Prof. Dr. I. Hermans University of Wisconsin – Madison, Department of Chemistry, 1101 University Avenue, Madison WI 53706, USA

\*hermans@chem.wisc.edu; Twitter: @hermansgroup

[b] Dr. S. Nagy, Dr. B. F. M. Kimmich

LyondellBasell Industries, Houston Technology Center, 8450 Sheldon Rd, Houston, TX 77049 USA

[c] Prof. Dr. I. Hermans

University of Wisconsin – Madison, Department of Chemical and Biological Engineering, 1415 Engineering Drive, Madison WI 53706, USA

#### **Abstract**

In this contribution we investigate the aerobic propylene epoxidation over a Ag/KNO<sub>3</sub>/CaCO<sub>3</sub> catalyst. The catalytic performance and surface speciation of the catalyst depends on the concentrations of feed modifiers such as ethyl chloride and nitric oxide, added to the feed to improve the selectivity by suppressing total combustion to CO<sub>2</sub>. After a kinetic characterization of the system, we investigate the kinetics in the presence of CO<sub>2</sub>. We demonstrate that CO<sub>2</sub> alters the rate dependence in both reactants, affects the activation of O<sub>2</sub>, and results in the same maximum rate of propylene oxide formation.

## Introduction

Propylene oxide (PO) is an important platform chemical with a worldwide demand that is currently exceeding 10 Mt/year. Applications rang across a vast number of industrial and consumer goods.<sup>[1–3]</sup> With all commercially practiced PO processes utilizing peroxides as the oxygen source, direct aerobic epoxidation of propylene is a transformation of great industrial interest and successful implementation of this process would present an important step forward.<sup>[4–7]</sup> However, the current

selectivity is too low to supersede state-of-the-art technologies, due to side reactions such as the overoxidation to CO<sub>2</sub>.<sup>[8]</sup>

Over the past 40 years, several studies improved our understanding of a variety of aerobic propylene epoxidation catalysts. The most promising, and hence best studied systems are silverbased, inspired by the industrial ethylene oxide production. The selectivity towards PO can be increased by feed modifiers and catalyst promoters. Nevertheless, our understanding of these complex but highly relevant systems, is still quite lacking and arguably is what has hindered the improvement of this reaction for industrial implementation. Many studies have been reported on silver-based catalysts for propylene epoxidation investigating, separately, support effects, promoters, and feed modifiers. Additionally, several investigations have been performed on controlled silver surfaces, including both experimental and computational work, to understand the possible mechanism for Ag-catalyzed propylene epoxidation. Unfortunately, the reaction has never been rigorously studied using industrially relevant conditions.

Two different mechanisms have been proposed based on evidence from model systems. Carter and Goddard first presented their oxyradical mechanism in 1988, proposing an Eley-Rideal mechanism in which a propylene molecule reacts from the gas phase with a surface activated oxygen atom to generate a surface bound propylene oxide product (Figure 1). Later, Linic and Barteau proposed a Langmuir-Hinshelwood mechanism based on computational data analogous to their prior computational work on ethylene epoxidation (Figure 2).<sup>[20–22]</sup> This pathway was investigated both computationally by Alonso and coworkers<sup>[17,18]</sup> and experimentally over Ag (111) and Ag (100) facets by Corma and coworkers.<sup>[15]</sup>

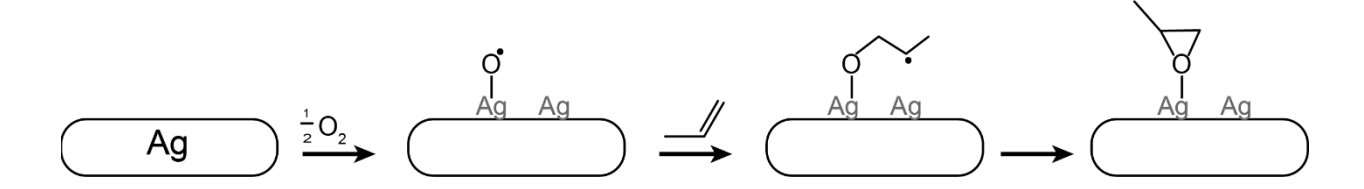


Figure 1. Proposed oxyradical propylene epoxidation mechanism over Ag(111) facets.

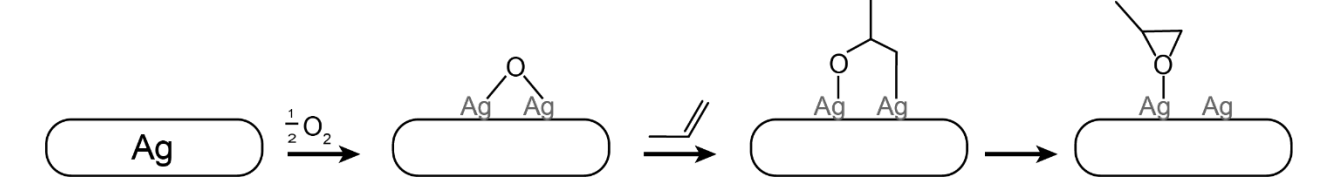


Figure 2. Proposed oxametallacycle propylene epoxidation mechanism over Ag(111) or Ag(100) facets.

Despite previous studies, to date, no kinetic data supporting either mechanism has been reported. Additionally, no study as of yet has looked at a complex system in its entirety to understand how components of the catalyst system combine to yield high selectivity at relevant conversions.

Herein, we seek to understand a complex propylene epoxidation catalyst system via a combined catalyst characterization, reactivity, and reaction kinetic analysis approach. The obtained insights could then potentially be used to improve our understanding of such systems and move towards industrial viability. Silver based catalytic systems that are commercially used for aerobic ethylene epoxidation and many catalysts that have been proposed for potential industrial application in aerobic propylene epoxidation contain a complex set of conditions in addition to the catalyst, including feed modifiers (*e.g.* alkyl chlorides) and various catalyst promoters (*e.g.* alkali metal salts, transition metal salts). [23,24,33-40,25-32] Ag/KNO<sub>3</sub>/CaCO<sub>3</sub> is a classic catalyst of interest for propylene epoxidation. Since it was first reported in the patent literature in the 1990s, [40] it has been the subject of numerous reports on various aspects of the catalyst system. [11,14,41] Several reports have commented on the industrial requirements for PO production, suggesting that in order

to be considered for industrial viability, a system must provide greater than 70% selectivity at 10% conversion. Although the currently attainable PO yields over this catalyst are still too low to be industrially viable, this system is a reasonable model in which to study the effects of multiple variables on the reactivity and reaction kinetics. To understand the system in total, this work accounts for the catalyst itself as well as feed modifiers (EtCl, NO) and a catalyst promoter (KNO<sub>3</sub>) that have been reported in the patent literature as an effective combination but to date have not been studied in combination with one another. Feed modifiers, such as alkyl chlorides and NO<sub>x</sub> species, are essential to maintaining high selectivity in propylene epoxidation according to several reports. Inc. 24,40,43–49 Therefore, we chose to include EtCl and NO as representative feed modifiers under catalytic conditions reported herein.

Of particular importance is an understanding of the reaction kinetics under realistic conditions. In ethylene epoxidation, the presence of catalyst promoters and feed modifiers has a dramatic effect on the reaction kinetics. For example, it was shown through fundamental surface science studies on Ag surfaces that the reaction order in O<sub>2</sub> or C<sub>2</sub>H<sub>4</sub> can vary widely depending on the inclusion of alkyl chloride feed modifiers. Recently, a microreactor study of ethylene epoxidation over silver microplates demonstrated reaction orders of 1 and 0.5 for O<sub>2</sub> and C<sub>2</sub>H<sub>4</sub> respectively, in the absence of feed modifiers. In 2018, it was shown that in an industrially relevant catalyst (Ag/ $\alpha$ -Al<sub>2</sub>O<sub>3</sub>), the reaction orders in O<sub>2</sub> and C<sub>2</sub>H<sub>4</sub> depend on the amount of Cl deposited on the surface during the reaction, where more chloride increases the reaction order in O<sub>2</sub> up to a maximum of 1, and diminishes the reaction order in C<sub>2</sub>H<sub>4</sub> from 0.5 to sub-zero. The clear importance of feed modifiers and promoters in alkene epoxidation makes kinetic studies under such conditions of vital importance.

In addition to the study of a complex system in itself, we also set out to explore the effects of CO<sub>2</sub> cofeeding in the system. The inclusion of CO<sub>2</sub> in the feed was proposed in the patent literature to improve the selectivity of epoxidation, despite CO<sub>2</sub> being the undesired byproduct. [24,30,40,54] In fact, there exists a series of studies on CO<sub>2</sub> effects in ethylene epoxidation; [29,34,38,39,55] however, a fundamental study on the effects of CO<sub>2</sub> in propylene epoxidation is lacking. For this reason, we set out to understand the effect of CO<sub>2</sub> on the reaction kinetics for vapor phase propylene epoxidation over Ag/KNO<sub>3</sub>/CaCO<sub>3</sub>. The work presented herein provides a critical step forward in the understanding of complex aerobic propylene epoxidation catalyst systems through combined catalyst characterization, reactivity studies, and reaction kinetics in the context of a complex system.

## Results and discussion

# Ag/KNO<sub>3</sub>/CaCO<sub>3</sub> reactivity in propylene epoxidation

#### Catalyst synthesis and characterization

The Ag/KNO<sub>3</sub>/CaCO<sub>3</sub> catalyst used in this work is synthesized by a wet impregnation of Ag on CaCO<sub>3</sub> followed by a post-synthetic wet impregnation of the KNO<sub>3</sub> promoter salt. To mimic catalysts found in the patent literature, the silver loading in the final catalyst is 56 wt%, with a 1.5 wt% K loading, as determined by inductively coupled plasma-optical emission spectroscopy (ICP-OES). The presence of metallic silver particles was confirmed by powder X-ray diffraction (Figure 3) and transmission electron microscopy (TEM) (Figure 4). Particle size distributions were calculated using the TEM images, in which only particles up to ca. 50 nm were discernable in large numbers; the fresh catalyst Ag/KNO<sub>3</sub>/CaCO<sub>3</sub> had an average particle size of  $4.9 \pm 4.4$  nm. From the powder X-ray diffraction pattern, the average particle size overall can be calculated using the

Scherrer equation, which yields an average particle size of  $27.9 \pm 4.39$  nm for the same Ag/KNO<sub>3</sub>/CaCO<sub>3</sub> material. While the two methods each have their limitations in determining overall particle size, a comparison of the two methods clearly demonstrates that neither is able to yield a comprehensive particle size distribution. Indeed, it is clear from the disagreement in the methods and the TEM images themselves that the catalyst contains numerous particles much larger than accounted for in the particle size distributions, yielding a catalyst with a plethora of potential active sites for propylene epoxidation.

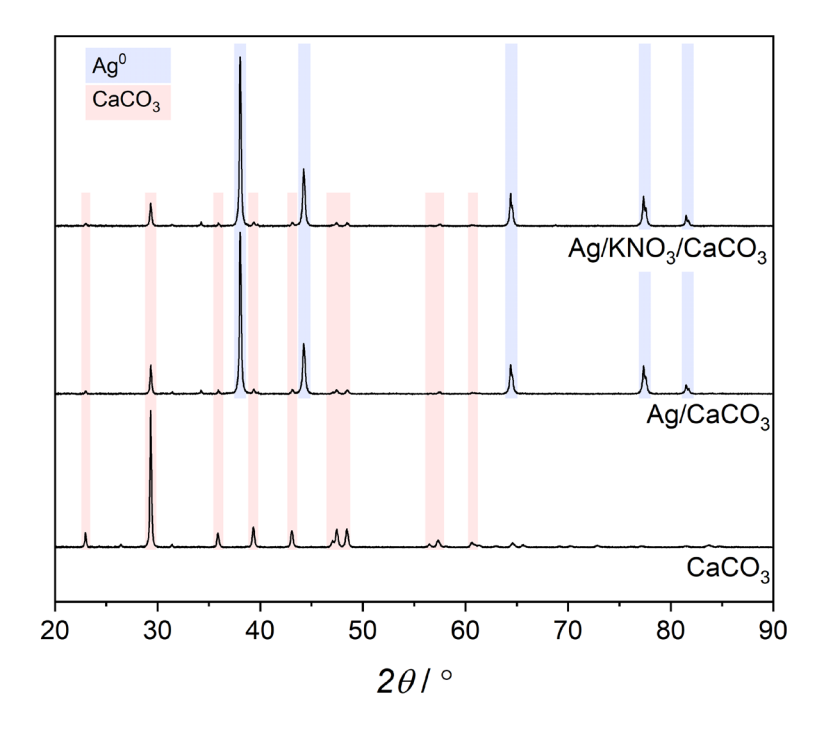


Figure 3. Powder X-ray patterns of CaCO<sub>3</sub> support, parent Ag/CaCO<sub>3</sub> catalyst, and KNO<sub>3</sub> treated catalyst. Major CaCO<sub>3</sub> reflections denoted in red, Ag<sup>0</sup> reflections denoted in blue.

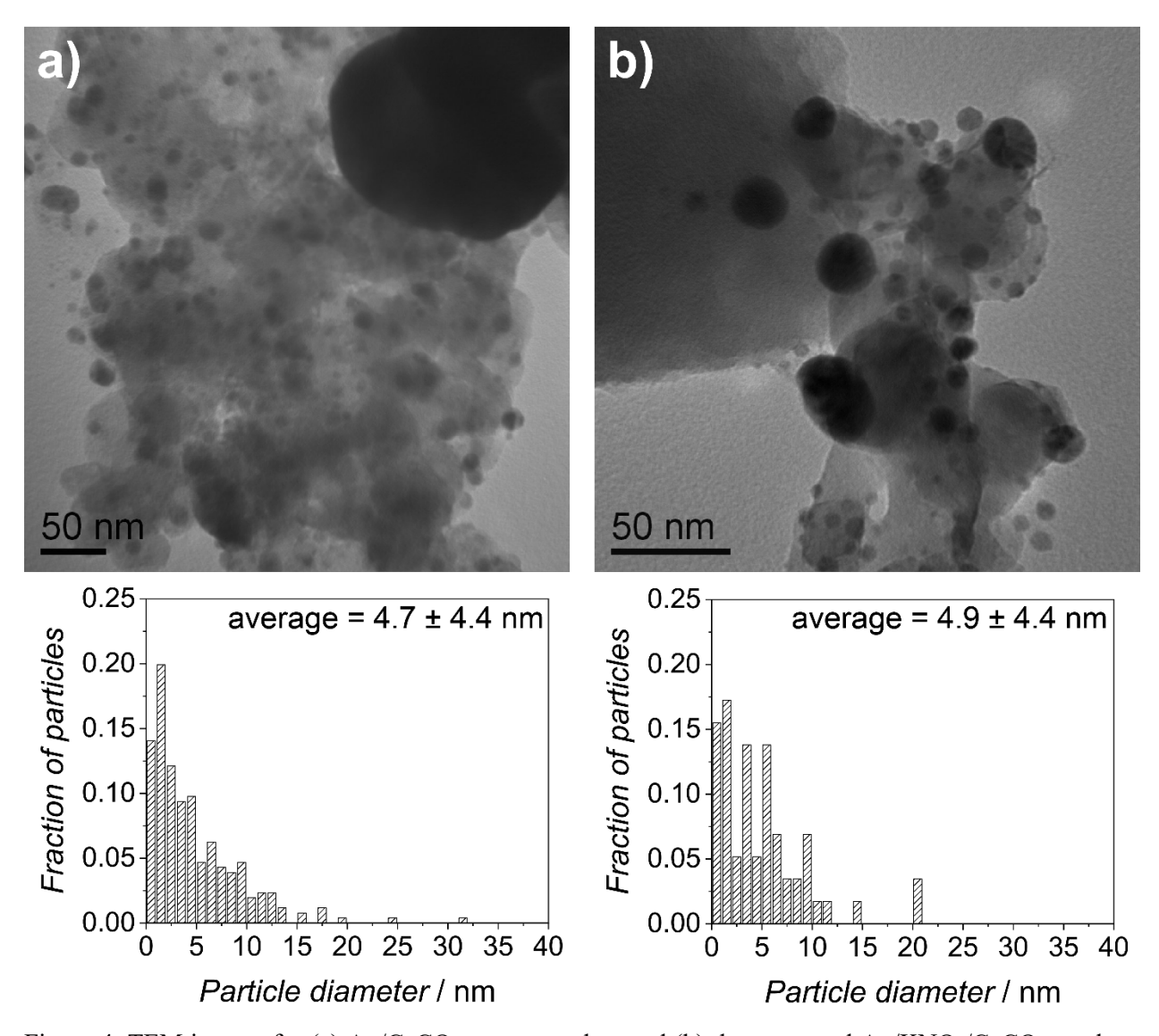


Figure 4. TEM images for (a) Ag/CaCO<sub>3</sub> parent catalyst and (b) the promoted Ag/KNO<sub>3</sub>/CaCO<sub>3</sub> catalyst. Corresponding particle size distributions and average particle diameters from TEM shown in histograms below each respective image.

# Catalyst reactivity and feed modifier effects

Prior to performing detailed kinetic measurements, we determined the selectivity and conversion of the catalyst system at intermediate concentrations in line with what is used in the patent literature (6% C<sub>3</sub>H<sub>6</sub>, 8% O<sub>2</sub>, 210 ppm EtCl, 70 ppm NO, balance N<sub>2</sub>) over a broad range of contact times using either 2 g or 500 mg of catalyst. These results include conversion and selectivity well outside of the differential regime useful for kinetic analysis (Figure 5), however, they indicate some

unusual catalytic behavior, namely the increase in epoxide selectivity at higher conversions. This result led to a thorough investigation of CO<sub>2</sub> cofeeding discussed in detail later. Under all conditions used in this study, the only observed products were PO and CO<sub>2</sub>, with carbon balances greater than 95% in all cases, and typically 98-100%.

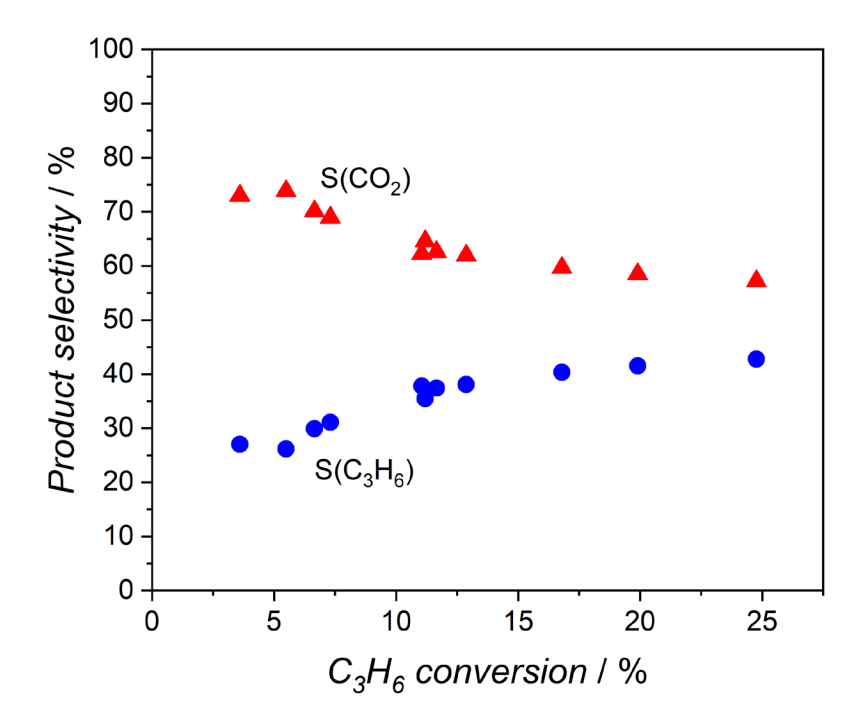


Figure 5. Product selectivity for propylene epoxidation over Ag/KNO<sub>3</sub>/CaCO<sub>3</sub> as a function of conversion; 2 g catalyst used for conversions greater than 10%, 500 mg catalyst used for conversions below 10%.

We observed that both EtCl and NO are necessary components of the reactant feed in order to achieve consistently high selectivity to PO. Previous reports examine the effects of alkyl chlorides on both ethylene and propylene epoxidation and found enhanced selectivity to propylene oxide (albeit typically at diminished rates of conversion in propylene epoxidation). Time course data for conversion and selectivity (Figure 6) reveal that when either EtCl or NO is removed, the selectivity decreases. In the case of EtCl removal, the conversion remains steady for several hours as the epoxide selectivity drops. After 12 hours, the epoxide selectivity is completely inhibited, while

conversion remains high. The catalyst selectivity immediately begins to recover after reintroduction of EtCl to the feed.

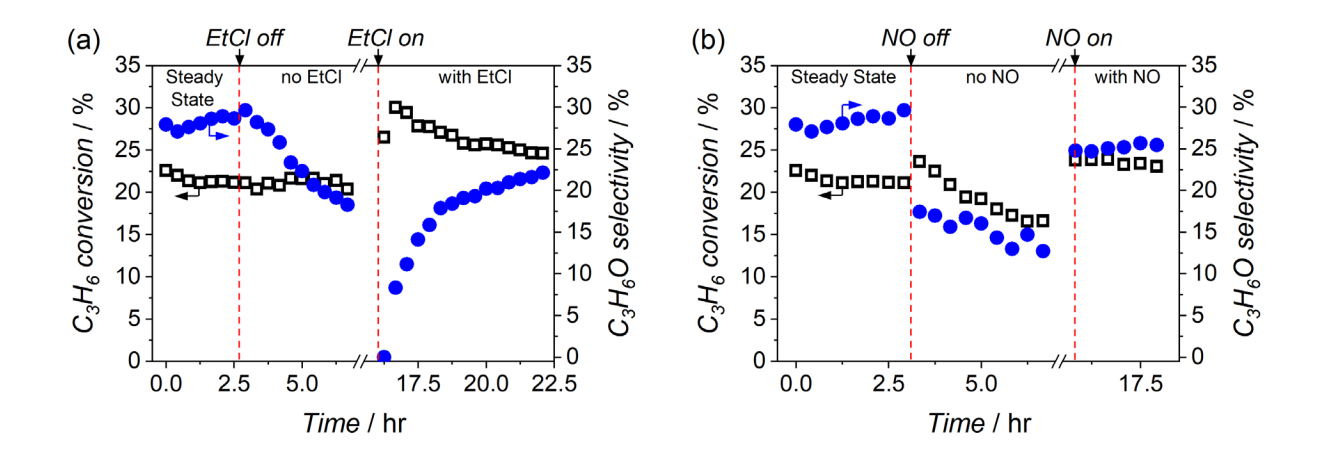


Figure 6. Time course data for steady state propylene epoxidation, followed by removal and replacement of feed modifiers (a) EtCl and (b) NO. Conditions: 255 °C,  $(C_3H_6) = 0.06$  bar,  $P(O_2) = 0.08$  bar, [EtCl] = 210 ppm, [NO] = 70 ppm.

Unlike EtCl, NO affects both the epoxide selectivity and propylene conversion; upon removal of NO from the feed, the epoxide selectivity and propylene conversion decrease over the course of several hours. After reintroduction of NO, the catalyst immediately recovers most of its activity. To better understand changes that may be occurring at the catalyst surface due to the presence of feed modifiers, we employed X-ray photoelectron spectroscopy (XPS) to perform surface elemental analysis of the catalyst before and after reaction. In addition, we performed epoxidation and subsequent XPS analysis over Ag/KNO<sub>3</sub>/CaCO<sub>3</sub> in the absence of one or both feed modifiers to understand the surface composition and the catalyst selectivity under different conditions. The XPS results and corresponding catalyst selectivity at steady state are reported in Table 1. We also evaluated the Ag particle size distribution after the reaction to discern whether any changes in particle size can be attributed to the presence of one or both feed modifiers (Figure 7). XRD and additional XPS data are provided in the supplemental information Figures S1 and Table S1.

Table 1. Surface composition of Ag/KNO<sub>3</sub>/CaCO<sub>3</sub> propylene epoxidation catalyst as a fresh catalyst and spent under various feed modifier conditions (Reaction condition) normalized to Ca content (determined by XPS), Ag particle size (determined by XRD) and corresponding epoxide selectivity at steady state reactivity. Total Ag content in all catalysts is the same (56 wt%), as determined by ICP-OES.

Reaction condition	Relative XPS elemental compositions							Ag	Epoxide	
	Ag	C (CO3 <sup>2-</sup> )	Ca	Cl	K	0	N	Mg	particle size (nm)	sel. (%)
Fresh catalyst	0.70	0.87	1.00	0.004	0.06	3.93	0.45	0.08	$27.9 \pm 4.4$	-
No modifiers	0.89	0.91	1.00	0.004	0.07	3.93	0.22	0.05	$26.2 \pm 5.1$	4.5
EtCl & NO	0.63	0.90	1.00	0.024	0.07	3.70	0.16	0.08	$26.9 \pm 5.2$	43
EtCl only	0.64	0.87	1.00	0.033	0.08	3.78	0.14	0.07	$27.8 \pm 5.1$	20
NO only	0.92	0.86	1.00	0.011	0.07	4.01	0.29	0.06	$25.7 \pm 4.7$	5.0

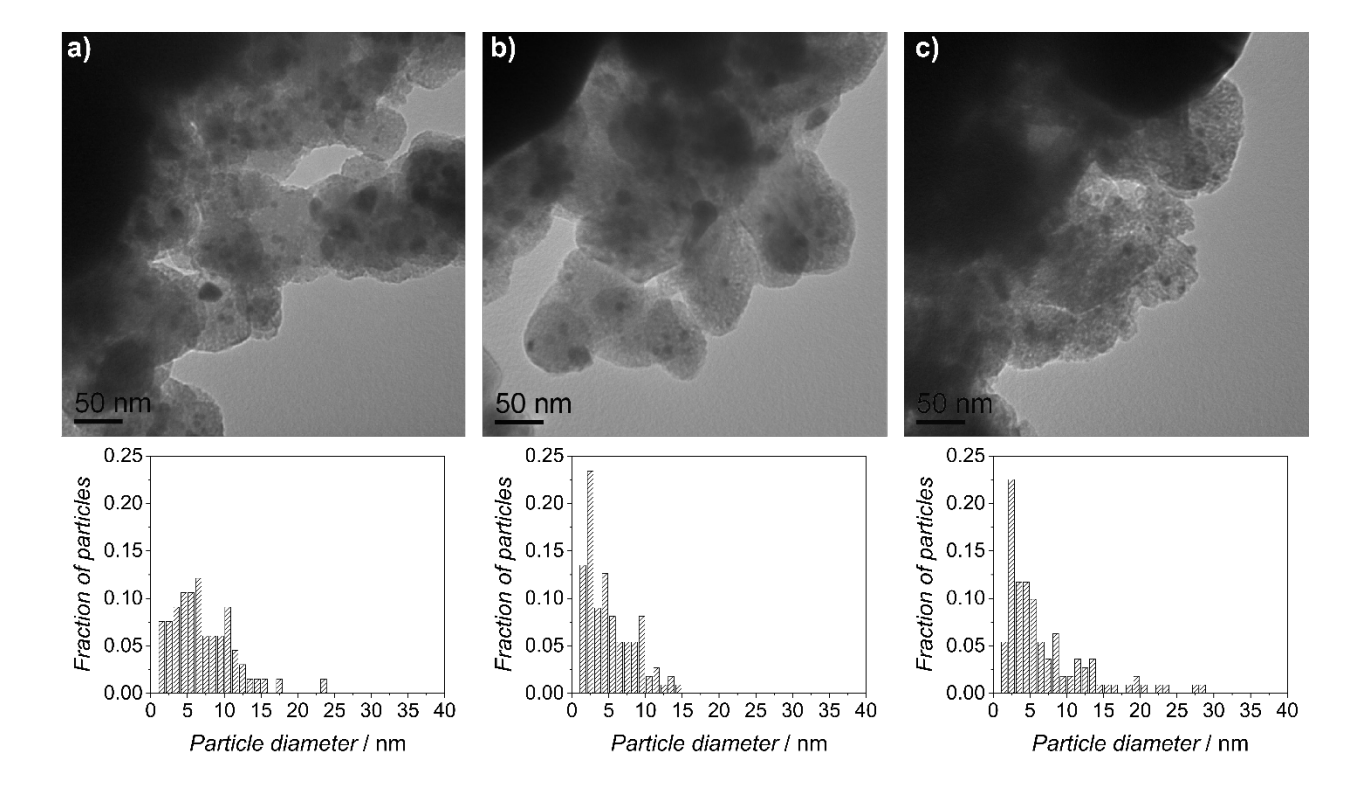


Figure 7. TEM images of Ag/KNO<sub>3</sub>/CaCO<sub>3</sub> after propylene epoxidation in the presence of different feed modifier compositions: (a) EtCl and NO, (b) EtCl, and (c) NO. Conditions:  $255 \,^{\circ}$ C,  $(C_3H_6) = 0.06$  bar,  $P(O_2) = 0.08$  bar, [EtCl] = 210 ppm, [NO] = 70 ppm.

The XPS data clearly indicate that the feed modifiers have a profound effect on the available surface species, particularly with respect to Ag, Cl and N composition. When no feed modifiers are present, the amount of Ag present at the surface increases by ca. 30% while the amount of surface N decreases compared to the fresh catalyst; under these conditions, the epoxide selectivity is only 4.5%. Meanwhile, inclusion of both EtCl and NO in the feed results in a similar surface silver content relative to the fresh catalyst along with higher epoxide selectivity (43%), indicating that the feed modifiers assist in moderating the available Ag surface sites, leading to increased selectivity. In fact, in the presence of EtCl with or without NO, the spent catalyst maintains a similar Ag surface loading relative to the fresh catalyst and higher epoxide selectivity than cases without EtCl at all. When the reaction is performed in the presence of EtCl, Cl is present in the surface composition of the final material, at either 0.33 or 0.43 atom % in the presence or absence of NO, respectively. XRD analysis of the spent material showed no detectable amounts of AgCl, indicating that the Cl is confined to the surface rather than migrating to the bulk. We postulate that the presence of Cl moderates the availability and activity of Ag surface sites by blocking Ag sites or altering the electronegativity of the Ag sites.

Based on the combination of XPS showing Cl incorporation and the time-on-stream data cycling EtCl inclusion / removal, and low but continuous levels of EtCl conversion throughout the reaction, we believe that Cl is continuously deposited on and removed from the surface during the reaction. This type of event would explain the continual conversion of EtCl and required presence of EtCl to maintain selectivity as well as the surface incorporation of Cl without the formation of bulk chloride species. Harris *et al.* recently reported on the fate of alkyl chloride species in the epoxidation of ethylene over  $Ag/\alpha$ - $Al_2O_3$ , in which Cl is deposited on the surface by a cofed alkyl chloride and subsequently removed *via* oxychlorination of ethane. [53,56] Similar chemistry likely

occurs in the propylene epoxidation system reported herein, although even with excellent overall mass balance, we were unable to detect oxychlorination products, likely due to concentrations below the detection limit.

The effect of cofed NO further convolutes the effects of EtCl in the feed. When only NO is included as a feed modifier, the catalyst selectivity and surface composition of the spent catalyst is quite similar to the case without feed modifiers. Specifically, the absence of NO leads to a higher silver surface coverage at ca. 12.5% rather than the ca. 9% found in the fresh catalyst and catalysts run in the presence of EtCl. Under those same conditions, the N content is lower than the fresh catalyst but higher than in the presence of EtCl. These surface changes do not seem to correlate with changes in particle size distribution or average particle size determined from XRD.

However, when EtCl and NO are present together, the improvement in selectivity is remarkable compared to the case with only NO and appreciable compared to the case with EtCl alone. The particle size distribution determined by TEM analysis exhibits the broadest distribution of particles in the range of 0-50 nm that we have yet observed, however the surface composition determined by XPS is relatively unchanged compared to the fresh catalyst, with the following two exceptions: inclusion of less Cl than the case with EtCl only and a significant decrease in the N content (from 6% in the fresh catalyst, to 2.5% under this condition). These data indicate a synergistic effect between EtCl and NO to maintain a higher catalyst selectivity through moderation of the catalyst surface. We hypothesize that EtCl and NO present in tandem aid in the rearrangement of Ag particles (through a possible sintering mechanism) and available surface species to yield more sites that are selective to epoxide. Due to the marked effect of feed modifiers on the catalyst surface speciation and selectivity, EtCl and NO were included at 210 ppm and 70 ppm, respectively, for

the remainder of the experiments in this work, although we acknowledge that further study of their molecular level effects would be of great value.

# Reaction kinetics to determine reaction rate dependence in C<sub>3</sub>H<sub>6</sub> and O<sub>2</sub>

After determining the initial reactivity of the catalyst, appropriate contact times were selected to yield kinetic data at concentrations up to 10% C<sub>3</sub>H<sub>6</sub> conversion. Oxygen consumption was typically less than 20% (although in some cases was as high as 38%), providing oxygen rich conditions for all kinetic experiments (even when P(O<sub>2</sub>) >> P(C<sub>3</sub>H<sub>6</sub>)). Reaction rate dependence in propylene was determined using partial pressures of 0.02-0.12 bar C<sub>3</sub>H<sub>6</sub> at a constant concentration of 10% O<sub>2</sub> (Figure 8). Reaction rate dependence in oxygen was determined using partial pressures of 0.02-0.12 bar O<sub>2</sub> with a constant C<sub>3</sub>H<sub>6</sub> concentration of 6% (Figure 9).

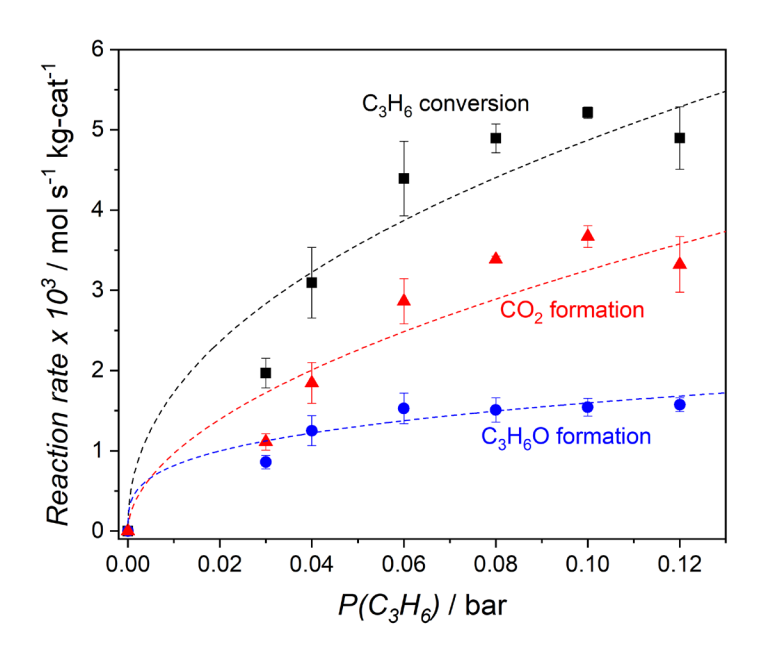


Figure 8. Reaction rate dependence on partial pressure of propylene. Conditions:  $255 \,^{\circ}\text{C}$ ,  $P(O_2) = 0.10 \,\text{bar}$ ,  $[NO] = 70 \,\text{ppm}$ ,  $[EtCl] = 210 \,\text{ppm}$ . Dashed lines are reaction rate fits.

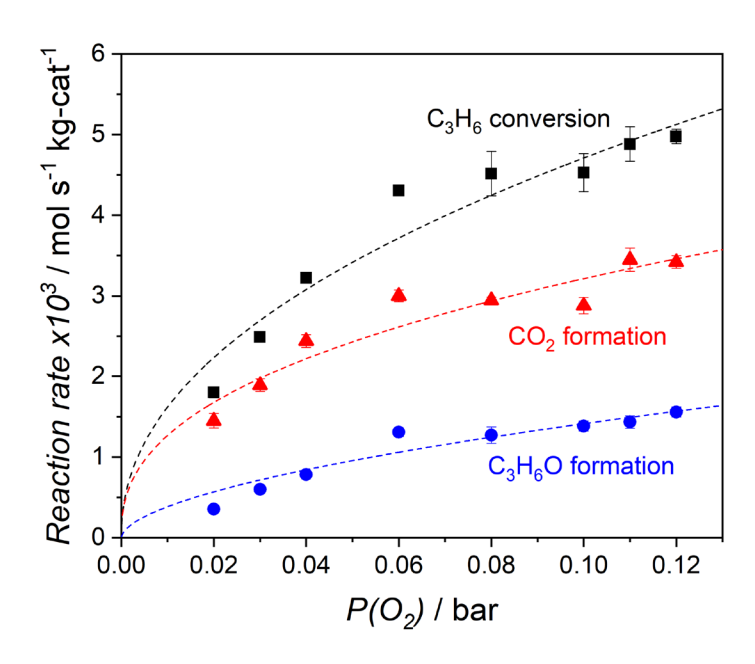


Figure 9. Reaction rate dependence on partial pressure of oxygen. Conditions: 255 °C,  $P(C_3H_6) = 0.06$  bar, [NO] = 70 ppm, [EtCl] = 210 ppm. Dashed lines are reaction rate fits.

The reaction rate shows adsorption dependence in both C<sub>3</sub>H<sub>6</sub> and O<sub>2</sub>, indicating a Langmuir-Hinshelwood mechanism in which both substrates must interact with the catalyst surface to react. Furthermore, both the rate of epoxide formation and the rate of CO<sub>2</sub> formation show adsorption dependence, indicating that there is no significant gas-phase reactivity contributing to the reaction, as might be expected if CO<sub>2</sub> was formed from a gas phase intermediate such as a propylene radical resulting from allylic H abstraction. Most importantly, this finding supports the hypothesis that the catalytic activity can be controlled by understanding and controlling the catalyst surface and does not depend strongly on the presence of uncontrolled gas-phase reactions.

It is important to note here that according to a Langmuir-Hinshelwood mechanism, we would expect the reaction rate to decrease at higher concentrations if the reactants are competing for the same site. The absence of this observation may therefore indicate that oxygen and propylene adsorb on slightly different surface sites within close proximity to one another. It is also possible

that high enough concentrations were not achieved under the experimental conditions used to observe a decline in reaction rate; the concentrations were chosen to minimize the possibility of generating an explosive mixture of propylene and oxygen.

## Effects of CO<sub>2</sub> cofeeding on propylene epoxidation

#### Reaction kinetics of cofed CO<sub>2</sub>

Based on the finding that selectivity improves with conversion, we chose to conduct a thorough investigation of CO<sub>2</sub> cofeeding. The CO<sub>2</sub> partial pressure in the feed was varied from 0 to 0.05 bar while holding C<sub>3</sub>H<sub>6</sub> and O<sub>2</sub> partial pressures constant (Figure 10). The overall rate of propylene conversion decreases, indicating CO<sub>2</sub> inhibits the reaction rate through surface adsorption. The reaction orders for propylene epoxidation are summarized in Table 2, giving the overall observed rate expressions in the last column of Table 2. Interestingly, conversion depends similarly on both propylene and oxygen (reaction orders of 0.45 and 0.46, respectively), while the individual product formation reactions have different dependencies. Epoxide formation has a reaction order of 0.57 in O<sub>2</sub>, compared with CO<sub>2</sub> formation which is 0.40 in O<sub>2</sub>. This trend is reversed, and more pronounced, for reaction orders in C<sub>3</sub>H<sub>6</sub>.

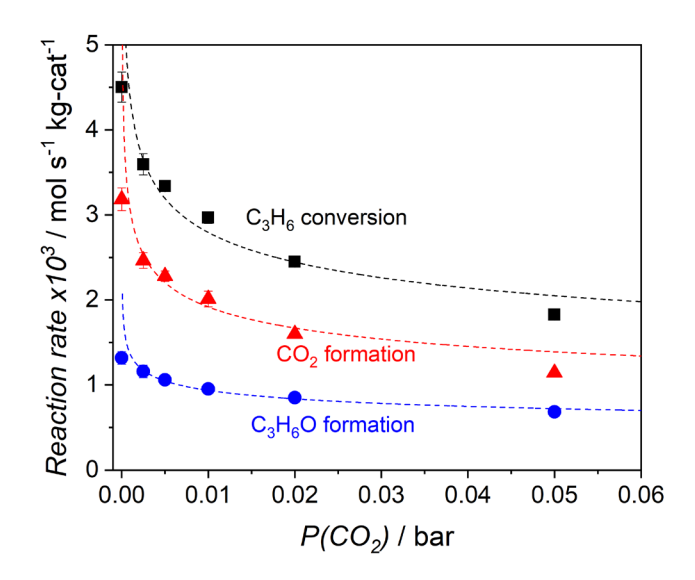


Figure 10. Reaction rate dependence on partial pressure of carbon dioxide. Conditions: 255 °C,  $P(O_2) = 0.08$  bar,  $P(C_3H_6) = 0.06$  bar, [NO] = 70 ppm, [EtCl] = 210 ppm, balance  $N_2$ . Dashed lines are reaction rate fits.

Table 2. Reaction orders in  $C_3H_6$ ,  $O_2$ , and  $CO_2$  partial pressures for product formation and propylene conversion. Calculated from reaction rate fits; errors in fits shown after  $\pm$  sign.

Reaction	Reaction order in C <sub>3</sub> H <sub>6</sub>	Reaction order in O <sub>2</sub>	Reaction order in CO <sub>2</sub>	Rate expression
C <sub>3</sub> H <sub>6</sub> O formation	$0.29 \pm 0.10$	$0.57\pm0.10$	$-0.16 \pm 0.03$	$\frac{k_{obs}[C_3H_6]^{0.29}[O_2]^{0.57}}{[CO_2]^{0.16}}$
CO <sub>2</sub> formation	$0.53 \pm 0.15$	$0.40\pm0.06$	$-0.20 \pm 0.01$	$\frac{k_{obs}[C_3H_6]^{0.53}[O_2]^{0.40}}{[CO_2]^{0.2}}$
C <sub>3</sub> H <sub>6</sub> conversion	$0.45\pm0.13$	$0.46\pm0.07$	$-0.19 \pm 0.03$	$\frac{k_{obs}[C_3H_6]^{0.45}[O_2]^{0.46}}{[CO_2]^{0.19}}$

Ultimately, the rate of CO<sub>2</sub> formation is inhibited more so than that of epoxide formation when CO<sub>2</sub> is included in the feed. This effect is most prominently observed in the selectivity to epoxide at iso-conversion (Figure 11a). At 5% CO<sub>2</sub> added, the selectivity to epoxide increases by 13% (*i.e.* from 26% to 39%) compared to the case in the absence of CO<sub>2</sub>.

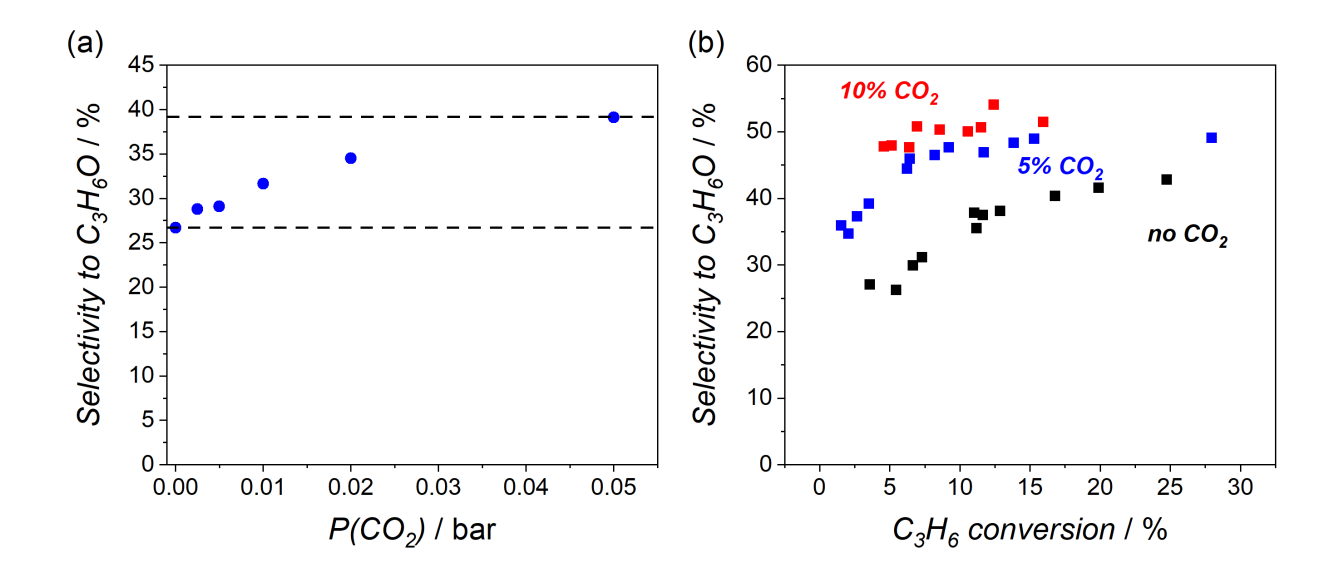


Figure 11. Propylene oxide selectivity during  $CO_2$  cofeeding (a) selectivity dependence as a function of  $CO_2$  concentration at constant  $C_3H_6$  conversion of 4% (dashed lines indicate upper and lower selectivity limits within the experiment), and (b) selectivity as a function of  $C_3H_6$  conversion at different  $CO_2$  concentrations. Reaction conditions: 255 °C,  $P(O_2) = 0.08$  bar,  $P(C_3H_6) = 0.06$  bar, [NO] = 70 ppm, [EtCl] = 210 ppm, balance  $N_2$ .

To determine whether the improved selectivity holds at higher conversions and higher CO<sub>2</sub> concentrations, the contact time was increased by increasing the catalyst loading in the reactor to 2 g for conversions above 10%. Propylene oxide selectivity remains enhanced at higher conversions at both 5 and 10% CO<sub>2</sub> and plateaus at higher maximum conversion (49 and 51%, respectively), as seen in Figure 11b. It appears that CO<sub>2</sub> cofeeding may be a viable way to improve reaction selectivity, although the productivity is diminished from 15 g C<sub>3</sub>H<sub>6</sub>O hr<sup>-1</sup> kg-cat<sup>-1</sup> in the absence of CO<sub>2</sub> to 8.8 g C<sub>3</sub>H<sub>6</sub>O hr<sup>-1</sup> kg-cat<sup>-1</sup> at 10% CO<sub>2</sub> added.

## Competitive reaction kinetics between CO<sub>2</sub> and C<sub>3</sub>H<sub>6</sub> or O<sub>2</sub>

Based on the finding that CO<sub>2</sub> exhibits a surface adsorption dependence in the reaction rate, we set out to understand where CO<sub>2</sub> adsorbs to the surface and whether it competitively adsorbs with C<sub>3</sub>H<sub>6</sub> or O<sub>2</sub>. We hypothesize that CO<sub>2</sub> likely interacts with oxygen on the surface, based on literature precedent showing CO<sub>2</sub> adsorbing to surface O<sub>a</sub> to generate surface carbonates.<sup>[57–60]</sup> The result of CO<sub>2</sub> interaction with surface oxygen sites should be an inhibition of oxygen to react with the surface due to site blocking by CO<sub>2</sub> and an overall decrease in the rate curves for propylene concentration dependence. To determine how CO<sub>2</sub> interacts with the surface in the presence of propylene and oxygen, we repeated the rate dependence in O<sub>2</sub> and C<sub>3</sub>H<sub>6</sub> while including 0.05 bar of CO<sub>2</sub>. These experiments place CO<sub>2</sub> in similar concentration to the substrates and therefore allows for observation of any competing behavior. The reaction rate dependencies are presented in Figure 12 and Figure 13 and a comparison of the reaction orders with and without CO<sub>2</sub> for C<sub>3</sub>H<sub>6</sub> and O<sub>2</sub> are presented in Table 3.

In the case of the C<sub>3</sub>H<sub>6</sub> concentration dependence with and without CO<sub>2</sub> (Figure 12), we found that the overall rates were diminished by the presence of CO<sub>2</sub>. This was expected based on the CO<sub>2</sub> rate dependence (Figure 10). The difference in formation rates for epoxide and CO<sub>2</sub> is much more apparent here than in the case of rate dependence on P(CO<sub>2</sub>); the dominant rate inhibition is due to a diminished rate of CO<sub>2</sub> formation, while the rate of epoxide formation achieves almost the same maximum value (1.5 *vs.* 1.2 mol(C<sub>3</sub>H<sub>6</sub>O) s<sup>-1</sup> kg-cat<sup>-1</sup>). Furthermore, the epoxide formation order in C<sub>3</sub>H<sub>6</sub> decreases to effectively zero, indicating that when CO<sub>2</sub> is present in similar concentration to C<sub>3</sub>H<sub>6</sub>, epoxide formation does not depend on C<sub>3</sub>H<sub>6</sub> concentration.

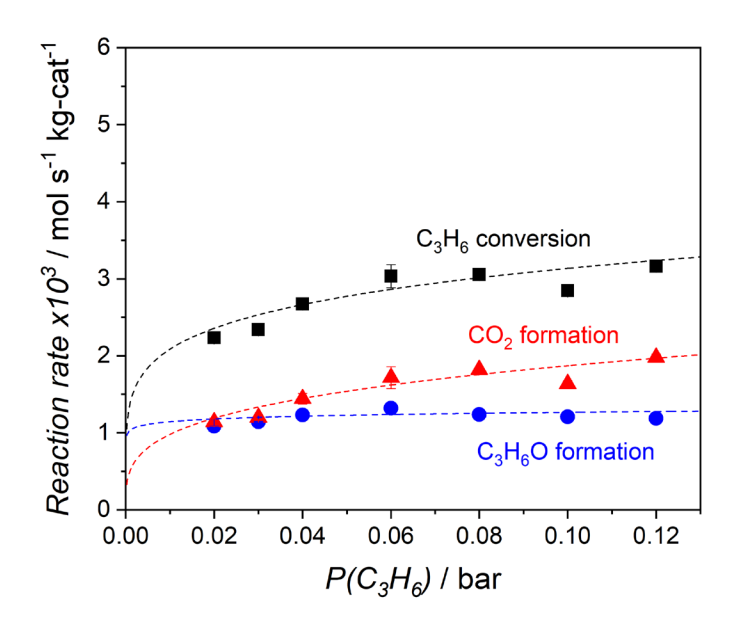


Figure 12. Reaction rate dependence on partial pressure of propylene in the presence of  $CO_2$ . Conditions: 255 °C,  $P(O_2) = 0.10$  bar,  $P(CO_2) = 0.05$  bar, [NO] = 70 ppm, [EtCl] = 210 ppm. Dashed lines are reaction rate fits.

In the case of rate dependence on P(O<sub>2</sub>) when 5% CO<sub>2</sub> is present in the feed, the behavior is quite different with and without CO<sub>2</sub> (Figure 13). The reaction remains first order to a higher concentration of O<sub>2</sub>; the reaction rate plateaus at a P(O<sub>2</sub>) of 0.12 as opposed to 0.06 in the absence of CO<sub>2</sub>. The rate of CO<sub>2</sub> formation is markedly affected, accounting for the majority of the decrease in the propylene conversion rate, similar to the competitive rate dependence experiment with C<sub>3</sub>H<sub>6</sub> (Figure 12). In addition, the rate of epoxide formation achieves the same maximum rate of 1.52 mol(C<sub>3</sub>H<sub>6</sub>O) s<sup>-1</sup> kg-cat<sup>-1</sup> when CO<sub>2</sub> is present as the case without CO<sub>2</sub> (1.48 mol(C<sub>3</sub>H<sub>6</sub>O) s<sup>-1</sup> kg-cat<sup>-1</sup>).

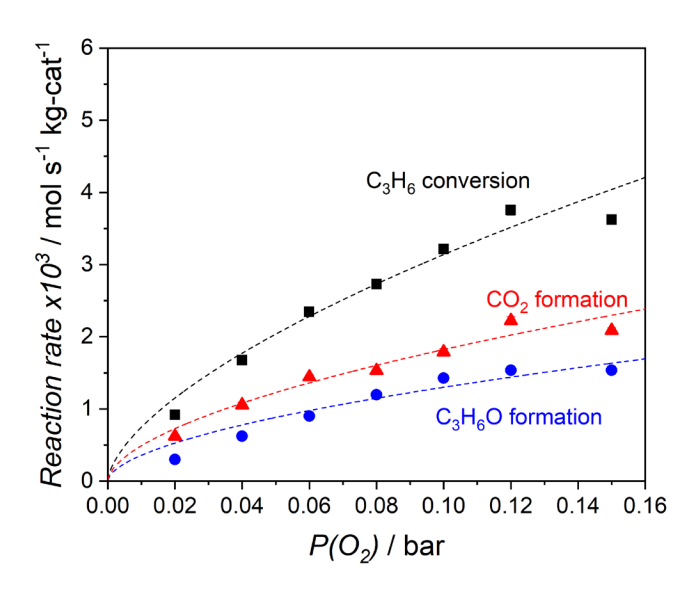


Figure 13. Reaction rate dependence on partial pressure of oxygen in the presence of  $CO_2$ . Conditions: 255 °C,  $P(C_3H_6) = 0.06$  bar,  $P(CO_2) = 0.05$  bar, [NO] = 70 ppm, [EtCl] = 210 ppm. Dashed lines are reaction rate fits.

When CO<sub>2</sub> is included in the feed at comparable concentrations to C<sub>3</sub>H<sub>6</sub> and O<sub>2</sub>, the reaction orders for epoxide and CO<sub>2</sub> formation change dramatically (Table 3). The reaction order in propylene for epoxide formation decreases from 0.29 to almost zero while the reaction order in O<sub>2</sub> remains the same. Meanwhile, for the formation of CO<sub>2</sub>, the reaction order in propylene is approximately halved (0.53 to 0.28) while the order in O<sub>2</sub> increases from 0.40 to 0.57, similar to that of epoxide formation under similar conditions.

Table 3. Reaction orders from calculated reaction rate fits without and with 0.05 bar  $CO_2$ . Error in fit shown after  $\pm$  sign.

Dogation	Reaction orde	r, CO <sub>2</sub> absent	Reaction order, CO <sub>2</sub> present		
Reaction	$C_3H_6$	$O_2$	$C_3H_6$	$O_2$	
C <sub>3</sub> H <sub>6</sub> O formation	$0.29 \pm 0.10$	$0.57 \pm 0.10$	$0.04 \pm 0.05$	$0.56 \pm 0.11$	
CO <sub>2</sub> formation	$0.53 \pm 0.15$	$0.40\pm0.06$	$0.28 \pm 0.06$	$0.57 \pm 0.08$	
C <sub>3</sub> H <sub>6</sub> conversion	$0.45 \pm 0.13$	$0.46 \pm 0.07$	$0.18 \pm 0.05$	$0.62 \pm 0.08$	

The findings from the competitive reaction kinetics indicate that CO<sub>2</sub> does not competitively adsorb with propylene or oxygen. If competitive adsorption occurred, we would expect to see a decrease in the maximum reaction rate in the presence of CO<sub>2</sub>. Instead, we postulate that CO<sub>2</sub> is adsorbing to surface oxygen sites that are unselective to epoxide but rather are selective to CO<sub>2</sub> as a product. The adsorption of CO<sub>2</sub> can form a carbonate, thus blocking the site and preventing the formation of CO<sub>2</sub>. This hypothesis explains why the decreased rate of CO<sub>2</sub> formation accounts for the majority of the decrease in conversion rate without affecting the maximum rate of epoxide formation. It also suggests that carbonate is more strongly adsorbed to the surface than the epoxide product, as the reaction order in O<sub>2</sub> is affected for both CO<sub>2</sub> and epoxide formation. Specifically, if carbonate does not desorb quickly enough, fewer surface sites are available for O<sub>2</sub> to dissociatively adsorb. The decrease is sites for O<sub>2</sub> adsorption leads to the slower transition from first order to second order in O<sub>2</sub> in the presence of CO<sub>2</sub>.

Reports in the ethylene epoxidation literature on the effects of CO<sub>2</sub> discuss the adsorption of CO<sub>2</sub> and formation of surface carbonate species. A series of studies by Bulushev and Khasin between 1985 and 1992 studied the effect of CO<sub>2</sub> inclusion in the feed stream for ethylene epoxidation at low pressures (1-400 Pa) over silver powder. Bulushev and Khasin found that (1) CO<sub>2</sub> generates surface carbonates during both the induction period and steady state reactivity and (2) the presence of CO<sub>2</sub> inhibits the rate of complete oxidation but does not affect the rate of selective oxidation. The difference in CO<sub>2</sub> dependence for the different oxidation pathways results in increased ethylene oxide selectivity in conjunction with a decrease ethylene conversion. Schouten *et al.* observed the same effect of elevated epoxide selectivity and lower overall reaction rate when cofeeding CO<sub>2</sub> under industrially relevant conditions: using an industrial Ag/ $\alpha$ -Al<sub>2</sub>O<sub>3</sub> catalyst and 2-10 bar total pressure. Other reports in the literature have examined the

pretreatment of Ag catalysts using CO<sub>2</sub> resulting in shorter induction periods or higher initial selectivity of the catalyst.<sup>[63]</sup> Based on the findings herein along with prior literature reports, we postulate that a similar phenomenon is occurring in our system for propylene epoxidation.

#### **Conclusions**

The results presented in this work using an industrially relevant system corroborate decades of computational and fundamental surface science studies that have proposed a Langmuir-Hinshelwood mechanism for propylene epoxidation on silver catalysts. While our work does not discuss the exact nature of the surface intermediates, it does provide a platform for future study of propylene epoxidation catalysts with different selectivity or activity.

Furthermore, we have presented the effects of CO<sub>2</sub> cofeeding in propylene epoxidation, demonstrating improved selectivity to PO in the presence of CO<sub>2</sub>. We observe that CO<sub>2</sub> predominantly suppresses the rate of CO<sub>2</sub> formation, resulting in improved PO selectivity. Furthermore, the effects of cofeeding of CO<sub>2</sub> can be extended to high concentrations of CO<sub>2</sub> (10% of the feed) and at high propylene conversions (>10%) to obtain improved PO selectivity at industrially relevant conversions.

# **Experimental**

## **Catalyst Synthesis**

Catalyst materials were prepared using previously reported procedures. [40] The catalyst loadings were confirmed by inductively coupled plasma-optical emission spectroscopy. Catalyst materials were prepared as follows: 0.37 mol of ethylene diamine (Sigma Aldrich, ReagentPlus >99%) was dissolved in 22.17 g of ultrapure water (resistivity = 18.2 M $\Omega$ ). The solution was heated to 50 °C

at which point 0.18 mol of oxalic acid dihydrate (Sigma Aldrich, ReagentPlus >99%) was slowly added, not allowing the temperature of the solution to exceed 60 °C. After the temperature stabilized ~50 °C, 0.18 mol of Ag<sub>2</sub>O (Sigma Aldrich, ReagentPlus >99%) was added along with 0.13 mol of ethanolamine (Sigma Aldrich, ReagentPlus >99%). The solution stirred for 30 minutes, at which point 0.28 mol of CaCO<sub>3</sub> (Specialty Minerals Inc.; Precipitated Calcium Carbonate, Vicality Light grade; > 98%) was added and mixed with a glass stirring rod until the paste was evenly mixed (approximately 20 minutes). The mixture was spread into calcination dishes to a thickness of ca. 0.25 cm, dried for 1 hour at 110 °C, then heated at 20 °C min<sup>-1</sup> up to 300 °C in a box furnace in air and held for four hours. The catalyst was removed from the oven and ground to a fine powder. In a subsequent step, the catalyst was mixed as a slurry into 150 mL of ultrapure water and KNO<sub>3</sub> (Sigma Aldrich; ReagentPlus, > 99%) was added (36.5 mmol per gram of catalyst). The slurry was stirred for 30 minutes, after which the water was removed by rotary evaporator at 60 °C followed by drying for 1 hour at 110 °C.

#### **Catalyst Characterization**

X-ray powder diffraction patterns were collected using a Bruker D8 Advance diffractometer outfitted with a Cu K $\alpha$  X-ray source and Lynxeye detector. Average particle sizes were calculated from the XRD patterns using peak fitting in Origin and the Scherrer equation. Silver and potassium loadings were measured by inductively coupled plasma-optical emission spectroscopy (ICP-OES) using a PerkinElmer Optima 2000 DV instrument after digestion in HNO<sub>3</sub>. Samples were prepared for TEM by sonicating  $\sim$  2 mg of sample in 2 mL of EtOH for 30 min to create a fine suspension then dipping a Cu grid with holey carbon backing (SPI supplies) into the suspension and allowing it to dry open to the air. TEM data were collected on a Tecnai T-12 transmission electron

microscope operated at 120 kV. Particles were measured and counted using ImageJ software. Between 100-150 particles were counted from each sample; the distributions were then normalized by reporting the fraction of total counted particles for each sample. Surface compositions were characterized by X-ray Photoelectron Spectroscopy (XPS) using a K-alpha XPS (Thermo Scientific) instrument with a micro-focused monochromatic Al Kα X-ray source. Samples were loaded into a Cu plate with multiple cavities for sample analysis. With multiple ports for sample loading on one plate, each sample could be measured under identical vacuum conditions. The samples were analyzed at 10<sup>-7</sup> mbar pressure and room temperature. Sample layers were greater than 1 mm thick, minimizing the effect from the Cu plate on the spectra. Charge was moderated by an electron gun in the instrument. The spectra in the C1s, O1s, N1s, K2p, Ag3d, C12p, Ca2p, and Mg1s regions were collected over multiple scans. The pass energy was held at 50 eV, the dwell time at 50 ms, and the energy step size at 0.2 eV for each region. Each region was integrated using the Avantage (Thermo Scientific) software package for determination of surface composition.

## **Catalyst Reactivity and Reaction Kinetics**

For reactivity and kinetic experiments, the catalyst bed was formed by first filling the bottom of a stainless steel (3/8" diameter) reactor tube with quartz wool and packing a quartz wool bed in the center of the reactor tube, then filling the appropriate amount of catalyst (500 mg or 2 g) directly on top of the quartz bed. The amount of quartz wool used to pack the reactor was adjusted for the amount of catalyst to ensure that the catalyst bed was centered vertically in the reactor tube. The tube was then loaded into a vertical split tube furnace (Carbolite) and connected to the gas feed. Gases were fed to the reactor through individual calibrated mass flow controllers (Bronkhorst) and the outlet of the reactor was fed through heated lines to an online gas chromatograph (Shimadzu GC-2010) outfitted with both a thermal conductivity detector (TCD) and flame ionization detector

(FID), as well as three Restek columns (RTX-1, RT-Msieve 5A, and Rt-Q-Bond). Feed gases consisted of O<sub>2</sub> (UHP, Airgas), C<sub>3</sub>H<sub>6</sub> (polymer grade, Airgas), 1000 ppm EtCl in N<sub>2</sub> (1077 ppm EtCl, balance N<sub>2</sub>; Airgas), 1000 ppm NO in N<sub>2</sub> (1024 ppm NO, balance N<sub>2</sub>; Airgas), either 5% CO<sub>2</sub> in N<sub>2</sub> (5.016% CO<sub>2</sub>, balance N<sub>2</sub>; Airgas) or pure CO<sub>2</sub> (99.999%, Airgas), and N<sub>2</sub> (UHP, Airgas) as a diluent.

The GC was calibrated using standard gas mixtures obtained from Airgas: 5% CO<sub>2</sub> in N<sub>2</sub>, 5% propylene, 5% ethylene, and 5% butene in N<sub>2</sub>, 0.4% propylene oxide in N<sub>2</sub>, 0.1% EtCl in N<sub>2</sub>, 10% and 2% O<sub>2</sub> in N<sub>2</sub>, 1% CO in N<sub>2</sub>. Gas mixtures or syringe injections of acrolein, propylene glycol, and acetone were also used during initial reaction method development but were never observed under reaction conditions. Nitric oxide was never observed in the GC in calibration, blank, or reaction measurements.

All reactions were performed at 255 °C, as monitored by a thermocouple in the reactor bed, and 1 bar pressure (concentrations are reported as vol% or partial pressure, interchangeably). Kinetic experiments were performed using 500 mg of catalyst and total flow rates between 60 and 160 mL min<sup>-1</sup>. High conversion reactions were performed using 2 g of catalyst and total flow rates between 40 and 160 mL min<sup>-1</sup>. The catalyst was conditioned under reactant flows of 6% C<sub>3</sub>H<sub>6</sub>, 8% O<sub>2</sub>, 210 ppm EtCl, and 70 ppm NO with a balance of N<sub>2</sub> for at least 12 hours to achieve steady state activity. Conversion was determined based on the total moles of C in the products (C<sub>3</sub>H<sub>6</sub>O and CO<sub>2</sub>) relative to the total moles of C in the reactant feed. Selectivity was determined by dividing the moles of C in one product by the total moles of C in the sum of the products. Carbon balance was 95% or greater, typically 98-100%.

# Acknowledgement

The authors acknowledge support from LyondellBasell Industries in funding this work. The authors acknowledge the use of transmission electron microscopy facilities and instrumentation supported by the National Science Foundation through the University of Wisconsin Materials Research Science and Engineering Center grant no. DMR-1720415.

**Keywords:** CO<sub>2</sub> cofeeding; epoxidation; propylene oxide; reaction kinetics; silver catalyst

#### References

- [1] J. H. Teles; I. Hermans; G. Franz; R. A. Sheldon. "Oxidation" in Ullmann's Encyclopedia of Industrial Chemistry, Wiley-VCH Verlag GmbH & Co. KGaA, Weinheim, 2015, pp. 1–103.
- [2] H. Baer; M. Bergamo; A. Forlin; L. H. Pottenger; J. Lindner. "*Propylene Oxide*" in *Ullmann's Encyclopedia of Industrial Chemistry*, Wiley-VCH Verlag GmbH & Co. KGaA: Weinheim, 2012; pp. 313–335.
- [3] K. Weissermel; H.-J. Arpe. "Propene Conversion Products" in Industrial Organic Chemistry, Wiley-VCH Verlag GmbH & Co. KGaA, Weinheim, 2003, pp. 267–312.
- [4] Technology Roadmap: Energy and GHG Reductions in the Chemical Industry via Catalytic Processes; 2013.
- [5] Energy and GHG Reductions in the Chemical Industry via Catalytic Processes: Annexes; 2013.
- [6] F. Cavani; J. H. Teles. *ChemSusChem* **2009**, *2* (6), 508–534.
- [7] T. A. Nijhuis; M. Makkee; J. A. Moulijn; B. M. Weckhuysen. *Ind. Eng. Chem. Res.* **2006**, 45 (10), 3447–3459.
- [8] S. J. Khatib; S. T. Oyama. Catal. Rev.: Sci. Eng. 2015, 57 (3).
- [9] S. Rebsdat; D. Mayer. "Ethylene Oxide" in Ullmann's Encyclopedia of Industrial Chemistry; Wiley-VCH Verlag GmbH & Co. KGaA, Weinheim, 2012, pp 547–572
- [10] G. Jin; G. Lu; Y. Guo; Y. Guo; J. Wang; X. Liu. React. Kinet. Catal. Lett. 2006, 89 (2), 253–260
- [11] J. Lu; J. J. Bravo-Suárez; M. Haruta; S. T. Oyama. Appl. Catal., A 2006, 302 (2), 283–295
- [12] A. Seubsai; M. Kahn; S. Senkan. *ChemCatChem* **2011**, *3* (1), 174–179
- [13] A. Takahashi; N. Hamakawa; I. Nakamura; T. Fujitani. Appl. Catal., A 2005, 294 (1), 34–

- 39.
- [14] F. W. Zemichael; A. Palermo; M. Tikhov; R. M. Lambert. *Catal. Letters* **2002**, *80* (May), 93–98.
- [15] A. Pulido; P. Concepción; M. Boronat; A. Corma. J. Catal. 2012, 292, 138–147.
- [16] E. A. Carter; W. A. Goddard III. *J. Catal.* **1988**, *112* (1), 80–92.
- [17] L. M. Molina; M. J. López; J. A. Alonso. *Phys. Chem. Chem. Phys.* **2014**, *16* (48), 26546–26552.
- [18] D. Torres; N. Lopez; F. Illas; R. M. Lambert. *Angew. Chem. Int. Ed.* **2007**, *46* (12), 2055–2058.
- [19] A. Kulkarni; M. Bedolla-Pantoja; S. Singh; R. F. Lobo; M. Mavrikakis; M. A. Barteau. *Top. Catal.* **2012**, *55* (1–2), 3–12.
- [20] S. Linic; M. A. Barteau. J. Am. Chem. Soc. 2003, 125, 4034–4035.
- [21] S. Linic; M. A. Barteau. J. Am. Chem. Soc. 2002, 124 (2), 310–317.
- [22] S. Linic; M. A. Barteau. *J. Catal.* **2003**, *214* (2), 200–212.
- [23] B. Cooker; A. M. Gaffney; J. D. Jewson; A. P. Kahn; R. Pitchai (Arco Chemical Technology), 5770746, 1998.
- [24] B. Cooker; A. M. Gaffney; J. D. Jewson; W. H. Onimus (Arco Chemical Technology), 5780657, 1998.
- [25] L. I. Rubinstein; C. Gutierrez (Shell Oil Company), 7153987B2, 2006.
- [26] G. W. Sears, Jr. (Dupont), 2615900, **1952**.
- [27] M. M. Bhasin; P. C. Ellgen; C. D. Hendrix (Union Carbide Chemicals and Plastics Company), 4916243, **1990**.
- [28] J. E. Buffum; R. M. Kowaleski; W. H. Gerdes (Shell Oil Company), 5145824, 1992.
- [29] S. B. Cavitt (Texaco), 4321206, **1982**.
- [30] B. Cooker; A. M. Gaffney; J. D. Jewson; A. P. Kahn (Arco Chemical Technology), 5856534, 1999.
- [31] A. M. Gaffney (Arco Chemical Technology), 5864047, **1999**.
- [32] W. H. Gerdes; J. R. Lockenmeyer; D. J. Remus; T. Szymanski; R. C. Yeates (Shell Oil Company), 8357813B2, **2013**.
- [33] P. Hayden; H. Pinnegar (Imperial Chemical Industries), 5011807, 1991.
- [34] P. Hayden; H. Pinnegar (Imperial Chemical Industries), 5099041, 1992.
- [35] A. P. Kahn; A. M. Gaffney (Arco Chemical Technology), 5861519, **1999**.
- [36] A. P. Kahn; A. M. Gaffney; R. Pitchai (Arco Chemical Technology), 5763630, 1998.

- [37] J. R. Lockemeyer; R. C. Yeates; D. Reinalda (Shell Oil Company), 8148555 B2, 2012.
- [38] M. Mitsuhata; F. Watanabe; T. Kumazawa (Nippon Shokubai Kagaku Kogyo Co.), 4368144, **1983**.
- [39] M. Nakajima; H. Kuboyama; T. Komiyama; H. Kimura; K. Yoshia (Mitsui Toatsu Chemicals), 4831162, **1989**.
- [40] R. R. Pitchai; A. P. Kahn; A. M. Gaffney (Arco Chemical Technology), US5625084A, 1997.
- [41] J. Lu; J. J. Bravo-Suárez; A. Takahashi; M. Haruta; S. T. Oyama. J. Catal. **2005**, 232 (1), 85–95.
- [42] S. Aldrett; A. van Mourik; R. Sebesta. Techno Economic Assessment of a Direct Route to Propylene Oxide. In *AIChE Annual Meeting*; Pittsburgh, 2012.
- [43] E. L. Force; A. T. Bell. J. Catal. 1976, 44, 175–182.
- [44] J. R. Monnier; J. L. Stavinoha; G. W. Hartley. J. Catal. 2004, 226 (2), 321–333.
- [45] T. C. R. Rocha; M. Hävecker; A. Knop-Gericke; R. Schlögl. J. Catal. 2014, 312, 12–16.
- [46] R. B. Grant; C. A. J. Harbach; R. M. Lambert; S. A. Tan; C. A. J Harbach; R. M. Lambert; S. Aun Tan. *J. Chem. Soc. Faraday Trans. I* **1987**, *83* (7), 2035–2046.
- [47] S. A. Tan; R. B. Grant; R. M. Lambert. J. Catal. 1987, 106, 54–64.
- [48] R. B. Grant; C. A. J. Harbach; R. M. Lambert; S. A. Tan. *J. Chem. Soc., Faraday Trans. 1* **1987**, *83* (7), 2035–2046.
- [49] W. Yao; X. Zheng; Y. Guo; W. Zhan; Y. Guo; G. Lu. J. Mol. Catal. A Chem. 2011, 342–343, 30–34.
- [50] C. T. Campbell; B. E. Koel. *J. Catal.* **1985**, *92*, 272–283.
- [51] C. T. Campbell. *J. Catal.* **1986**, *99*, 28–38.
- [52] T. Salmi; J. Hernández Carucci; M. Roche; K. Eränen; J. Wärnå; D. Murzin. *Chem. Eng. Sci.* **2013**, *87*, 306–314.
- [53] C.-J. Chen; J. W. Harris; A. Bhan. Chem. Eur. J. **2018**, 5 (6), 644–656.
- [54] P. Hayden; R. J. Sampson; C. B. Spencer; H. Pinnegar (Imperial Chemical Industries), 4007135, **1977**.
- [55] A. C.-Y. Liu; E. M. Thorsteinson; H. Soo; J. H. McCain; D. M. Minahan (Union Carbide Chemicals & Plastics Corporation), 6511938 B1, 2003.
- [56] J. W. Harris; A. Bhan. J. Catal. 2018, 367.
- [57] K. J. Maynard; M. Moskovits. J. Chem. Phys. 1989, 90 (11), 6668–6679.
- [58] X. C. Guo; R. J. Madix. J. Phys. Chem. B 2001, 105 (18), 3878–3885.
- [59] D. A. Bulushev; A. V. Khasin. *React. Kinet. Catal. Lett.* **1991**, 44 (2), 421–425.

- [60] D. A. Bulushev; A. V. Khasin. React. Kinet. Catal. Lett. 1991, 44 (2), 463-468.
- [61] D. A. Bulushev; A. V. Khasin. React. Kinet. Catal. Lett. 1991, 44 (2), 439-444.
- [62] E. P. S. Schouten; P. C. Borman; K. R. Westerterp. *Chem. Eng. Process.* **1996**, *35*, 107–120.
- [63] A. Aho; K. Eränen; L. J. Lemus-Yegres; B. Voss; A. Gabrielsson; T. Salmi; D. Y. Murzin. J. Chem. Technol. Biotechnol. 2018, 93 (6).

## **Table of Contents**

Catalyst systems used in propylene epoxidation are often lacking thorough understanding of the system due to the complex nature of the catalyst. Improving selectivity is a key goal for the future implementation of aerobic propylene epoxidation. The catalytic performance, reaction kinetics, and surface speciation were investigated for Ag/KNO<sub>3</sub>/CaCO<sub>3</sub> in propylene epoxidation in the presence of EtCl and NO feed modifiers. The effects of CO<sub>2</sub> cofeeding were also examined, with added CO<sub>2</sub> leading to higher propylene oxide selectivity.

